SUPPORTING INFORMATION

Unraveling Gibbsite Transformation Pathways into LiAl-LDH in Concentrated Lithium Hydroxide

Trent R. Graham,[*,†,‡] Jian Zhi Hu,[†,⊥,φ] Xin Zhang,[†] Mateusz Dembowski,[†] Nicholas R. Jaegers,[†,⊥,φ] Chuan Wan,[⊥] Mark Bowden,[†,#] Andrew S. Lipton,[#] Andrew R. Felmy,[†] Sue B. Clark,[€,§,‖] Kevin M. Rosso,[†] and Carolyn I. Pearce[*,€]

†Physical and Computational Sciences Directorate, Pacific Northwest National Laboratory, Richland, Washington 99354, United States

‡The Voiland School of Chemical and Biological Engineering, Washington State University, Pullman, Washington 99164, United States

⊥Institute for Integrated Catalysis, Pacific Northwest National Laboratory, Richland, Washington 99354, United States

φBiological Science Directorate, Pacific Northwest National Laboratory, Richland, Washington 99354, United States

#Environmental Molecular Sciences Laboratory, Pacific Northwest National Laboratory, Richland, Washington 99354, United States

€Energy and Environment Directorate, Pacific Northwest National Laboratory, Richland, Washington 99354, United States

§Department of Chemistry, Washington State University, Pullman, Washington 99164, United States

‖Materials Science and Engineering Program, Washington State University, Pullman, Washington 99164, United States

Corresponding Authors

*Trent R. Graham, E-mail: trenton.graham@pnnl.gov
*Carolyn I. Pearce, E-mail: Carolyn.pearce@pnnl.gov

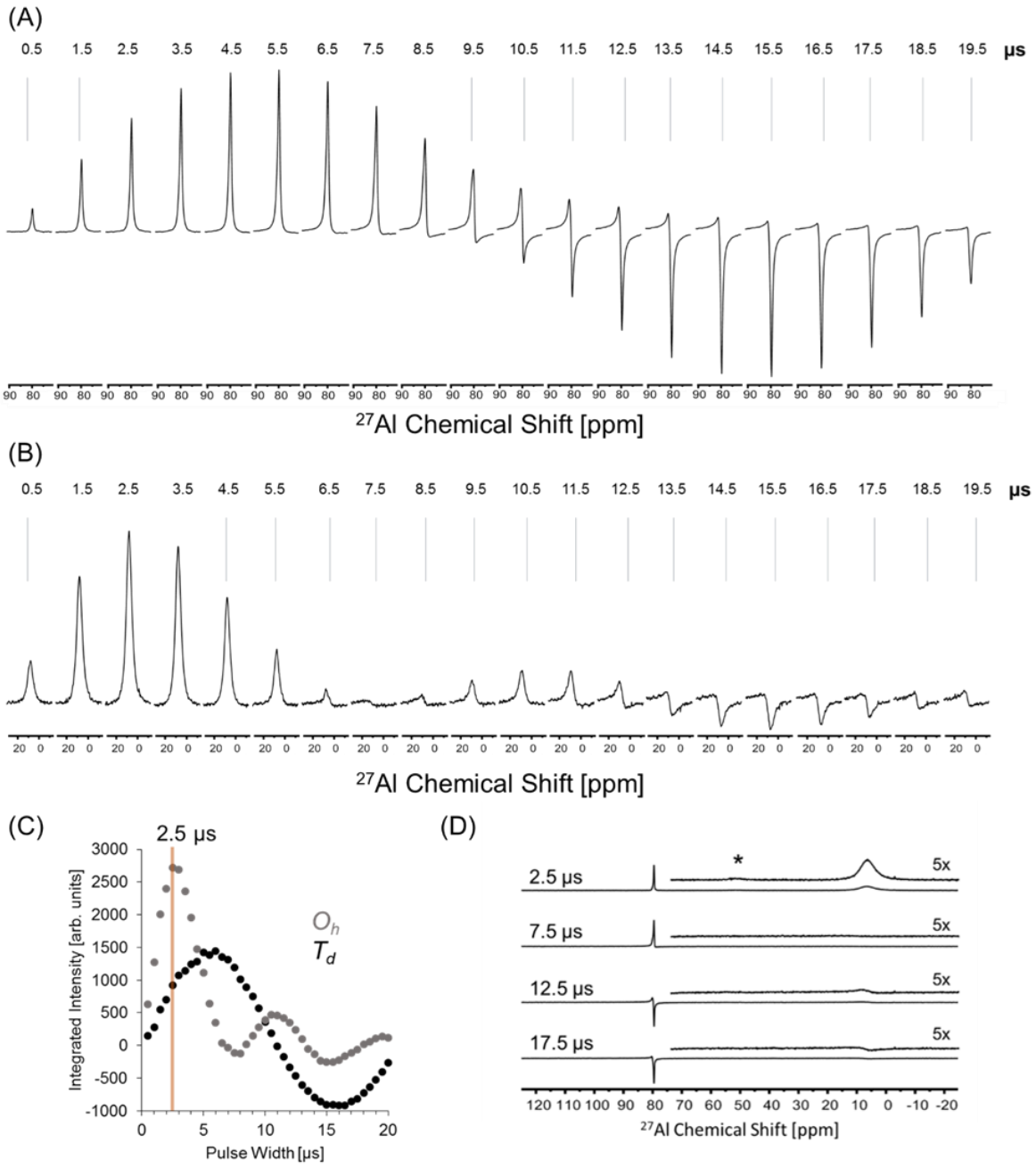

Figure S1. ^{27}Al MAS NMR spectra are shown at a field strength of 7.0 T, at a calibrated temperature of 25°C, using a 7.5 mm, magic angle spinning (MAS) probe operating with a spin rate of approximately 3.8 kHz. A single excitation pulse, a 1 s recycle delay time and an 80 ms acquisition time facilitated use as a pulse width (pw) nutation experiment. The excitation pulse width (duration in µs) is shown above each spectrum. (A) The tetrahedral (T_d) and (B) octahedral (O_h) ^{27}Al MASNMR resonance are shown. (C) The integrated ^{27}Al MAS NMR, center band intensities are plotted. (D) The spectra on a unified vertical scale, with a 5x vertical magnification of the O_h region offset. The asterisk marks the T_d Al spinning side band.

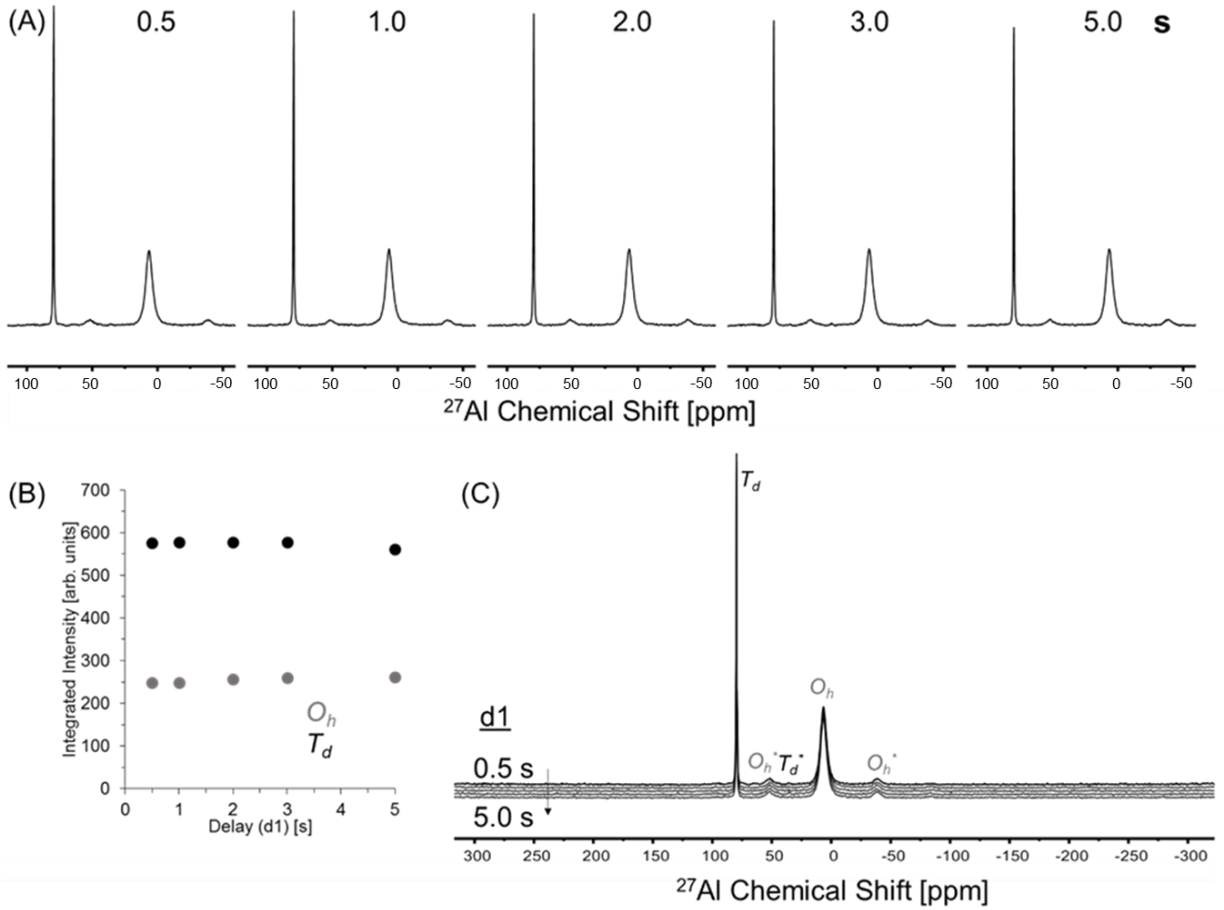

Figure S2. (A) ^{27}Al MAS NMR spectra are shown at 7.0 T, at a calibrated temperature of 25°C, using a 7.5 mm, magic angle spinning (MAS) probe operating at a spin rate of approximately 3.8 kHz. These spectra utilized a single 2.5 µs pulse (corresponding to a liquid π/4 pulse) and an 80 ms acquisition time - settings which facilitated use as a recycle delay (d1) nutation experiment. The d1 value (in seconds) is shown above each spectrum. (B) The integral of the center transition of the octahedral Al (O_h) and tetrahedral (*Td*) resonance are plotted. (C) The full spectral width of the spectra and ^{27}Al assignments are shown. O_h^* and T_d^* denote spinning side bands attributed to the O_h and T_d resonance, respectively.

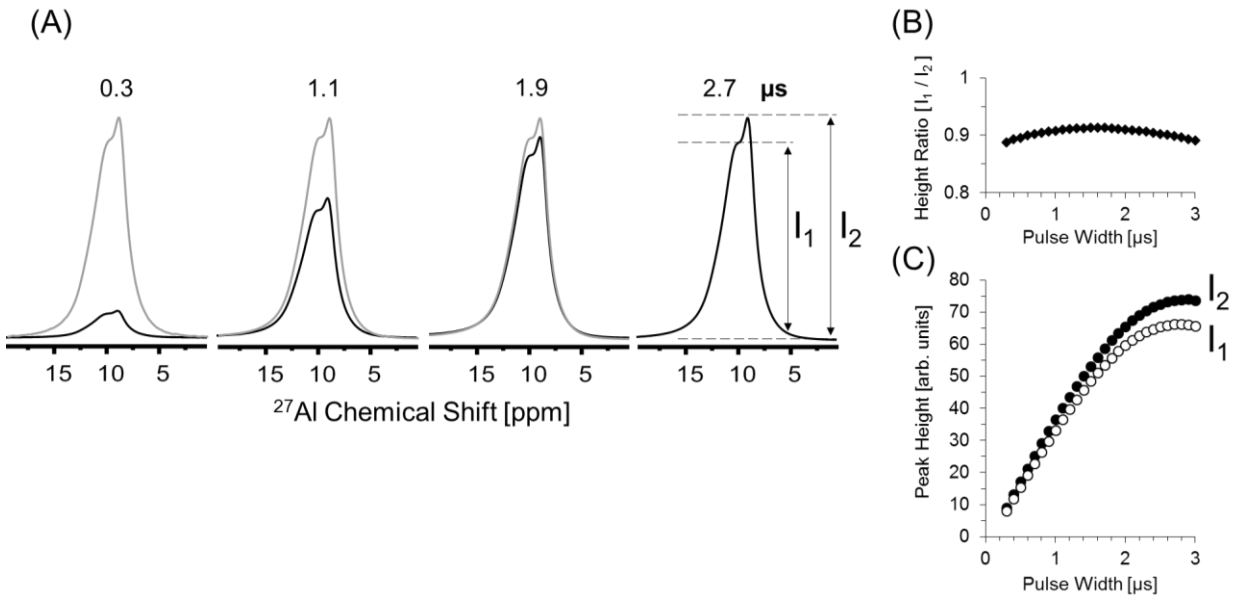

Figure S3. (A) ^{27}Al MAS NMR spectra are shown at 20.0 T, at 25 °C, using a 3.2 mm, magic angle spinning (MAS) probe operating at a spin rate of approximately 13.2 kHz. These spectra utilized a single excitation pulse, a recycle delay of 1 s, and a 100 ms acquisition time - settings which facilitated use as a pulse width (pw) nutation experiment. The pw value (in microseconds) is shown above each spectrum. Spectra in gray are vertically scaled to the same height. The analyzed line shape parameters (peak height denoted I_1 and I_2) are shown. For this sample, no signal intensity in the T_d region (80-70 ppm) nor the penta coordinated Al region was detected. The sample was prepared by vortex mixing 0.5 M gibbsite ($Al(OH)_3$) in 3 M LiOH in D_2O for 1 h in an N_2-filled glove box. The product was washed with D_2O three times using a centrifuge also located within the glovebox. The washed product was then dried for 3 days at room temperature and briefly ground with a mortar and pestle in the glovebox prior to NMR experiments. (B) The peak height ratio of I_1 and I_2 as a function of pulse length. (C) The peak heights of I_1 and I_2 as a function of pulse width. These results indicate that the use of an excitation pulse width corresponding to a $\pi/4$ tip angle at 20.0 T improves the signal to noise of spectra by a factor of ca. 5.6 (relative to the signal acquired with the same number of transients and a $\pi/20$ tip angle) with little effect on the line shape due to the reduction of quadrupolar 2nd order effects at high magnetic field strengths.

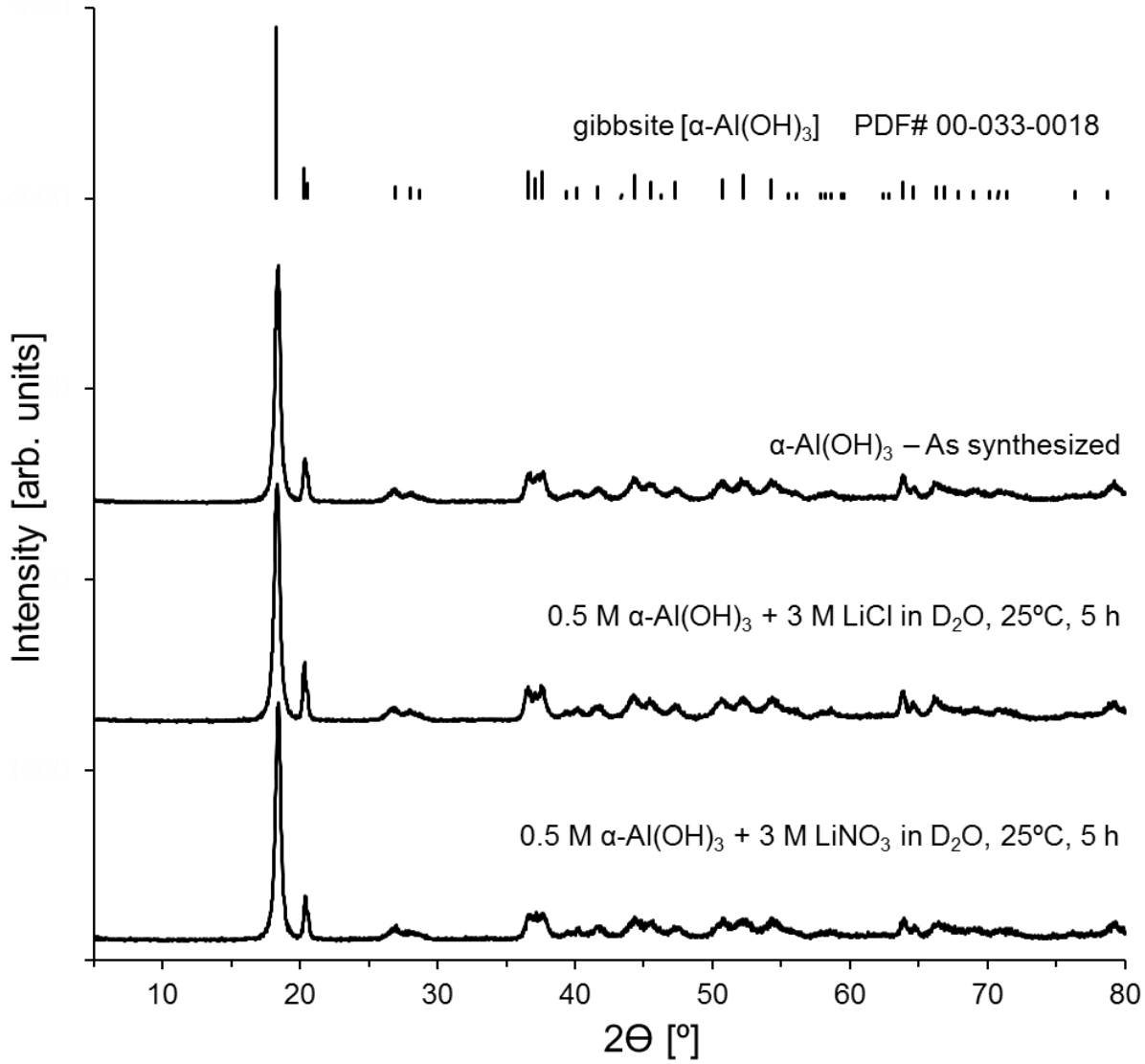

Figure S4. XRD patterns of gibbsite [α-$Al(OH)_3$], as synthesized and following dispersion of 0.5 M α-$Al(OH)_3$ in 3 M LiCl or 3 M $LiNO_3$ in D_2O at 25ºC for 5 h. The dispersed α-$Al(OH)_3$ were collected by centrifugation, washed with D_2O three times and dried in an oven at 50ºC. XRD patterns were acquired on a Philips X'pert Multi-Purpose diffractometer (MPD) (PANAlytical Almelo, The Netherlands), equipped with a fixed Cu anode operating at 40 mA and 50 kV. No Li^+ intercalated phase ($Li[Al(OH)_3)]_2Cl{\cdot}nH_2O$ or $Li[Al(OH)_3)]_2NO_3{\cdot}nH_2O$, or deuterated counterparts) appears in the XRD patterns following dispersion in 3 M LiCl or 3 M $LiNO_3$, respectively.

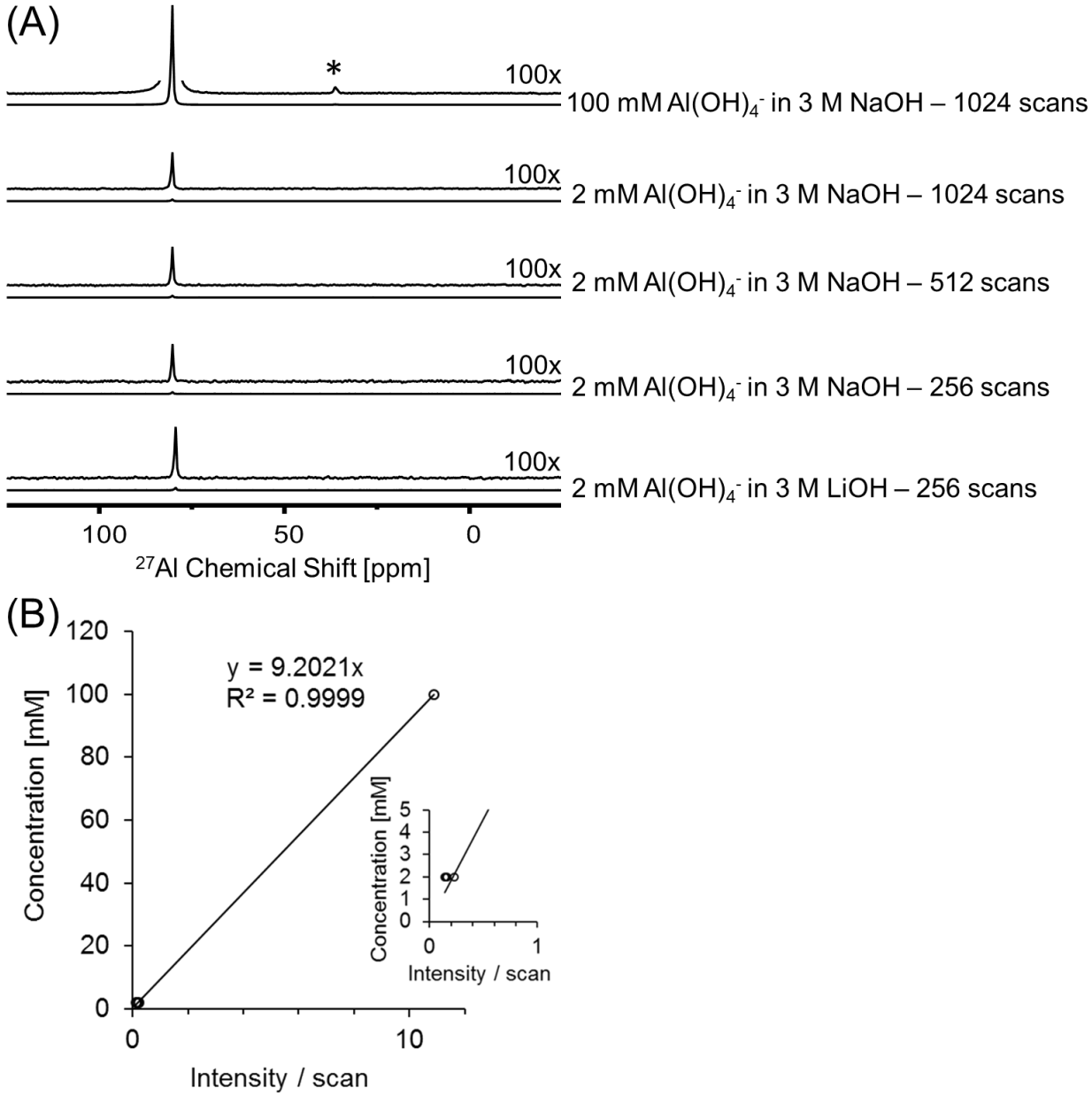

Figure S5. (A) ^{27}Al MAS NMR spectra collected at 7.0 T, at a calibrated temperature of 25°C, using a 7.5 mm MAS probe operating with a spin rate of approximately 3.8 kHz. Spectra were collected using a single 2.5 µs pulse, 80 ms acquisition time, and a 1 s recycle delay - settings which facilitated use as an external concentration reference for *in situ* ^{27}Al MAS NMR (see Figure 1 in the manuscript). Samples were prepared from the dissolution of gibbsite (α-$Al(OH)_3$), wherein gibbsite was loaded directly into the NMR rotor followed by addition of 3 M NaOH or LiOH in D_2O in a glovebox to prevent the sorption of CO_2. Scans are normalized by the number of transients and a spinning sideband is denoted with an asterisk (*). Scans magnified vertically by a factor of 100x are offset above the spectra. (B) The corresponding calibration curve and linear regression acquired from the integral of the center transition. The inset shows 4 data points corresponding to spectra of 2 mM $Al(OH)_4^-$.

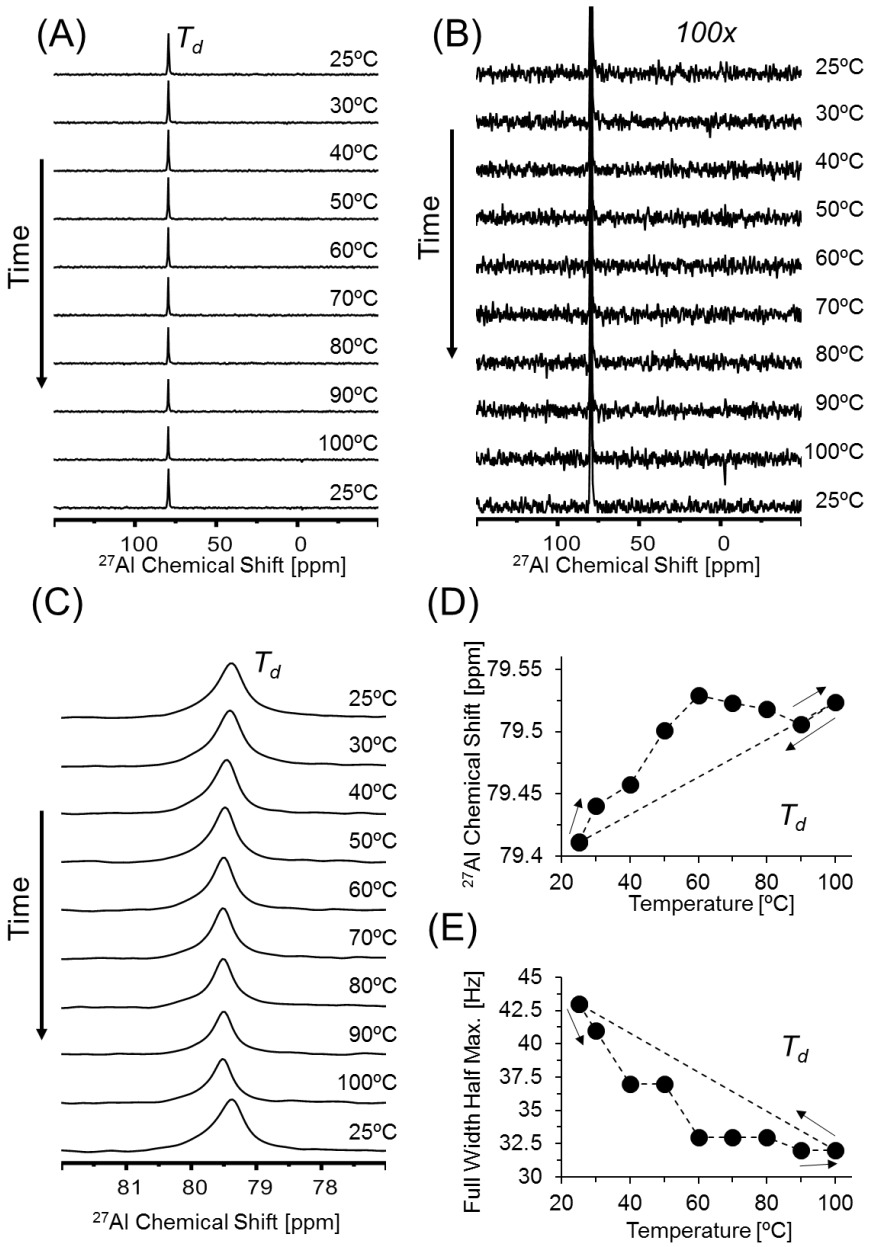

Figure S6. Variable temperature ^{27}Al MAS NMR spectra collected at 7.0 T, using a 7.5 mm MAS probe operating with a spin rate of approximately 3.8 kHz. Spectra were collected using a single 2.5 µs pulse, 80 ms acquisition time, and a 1 s recycle delay with 256 transients. The sample is 2 mM $Al(OH)_4^-$ in 3 M LiOH in D_2O. The sample was heated at approximately 3 ºC min^{-1}. (A) The acquired ^{27}Al NMR spectra (B) Vertical magnification of Figure S6A by a factor of 100. (C) Horizontal magnification of Figure S6A. (D) The peak position of the tetrahedral (T_d) peak pertaining to $Al(OH)_4^-$. (E) The full width half maximum of the T_d peak. In Figure S5 (D) and (E), the arrows delineate the temporal evolution of temperature and the dashed lines are drawn only to guide the eyes.

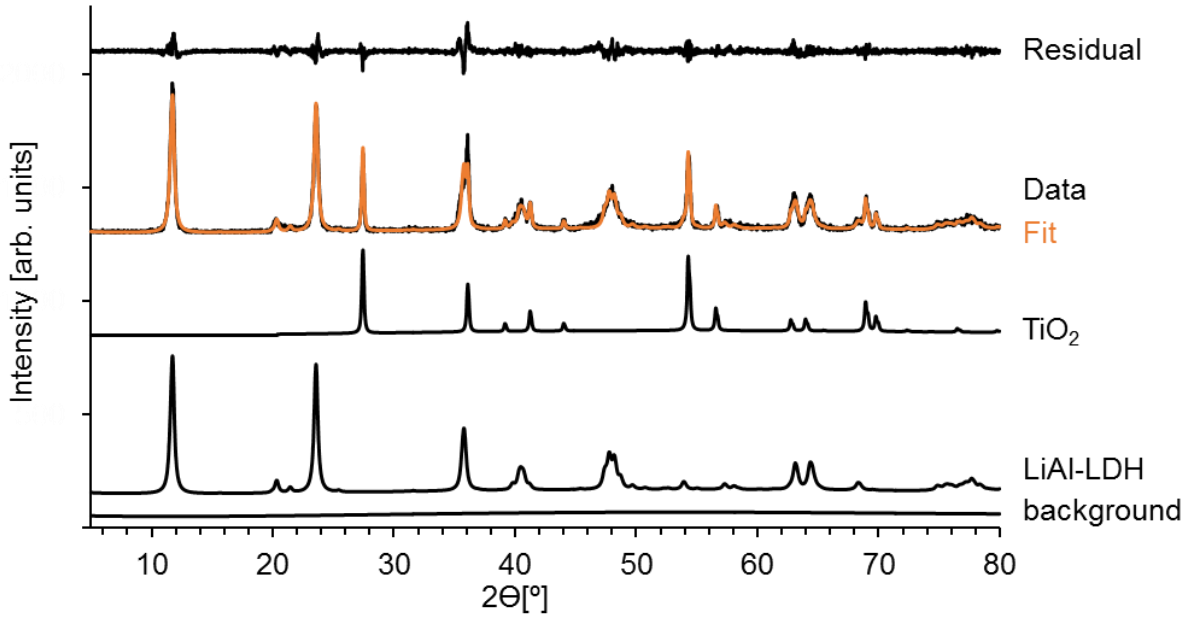

Figure S7. XRD patterns of LiAl-LDH [$Li(Al(OH)_3)_2OH{\cdot}2H_2O$] and TiO_2. The weight percent $Li(Al(OH)_3)OH{\cdot}2H_2O$ is 78.5 %. XRD patterns were acquired on a Philips X'pert Multi-Purpose diffractometer (MPD) (PANAlytical Almelo, The Netherlands), equipped with a fixed Cu anode operating at 40 mA and 50 kV. The fit was produced in TOPAS (v5).

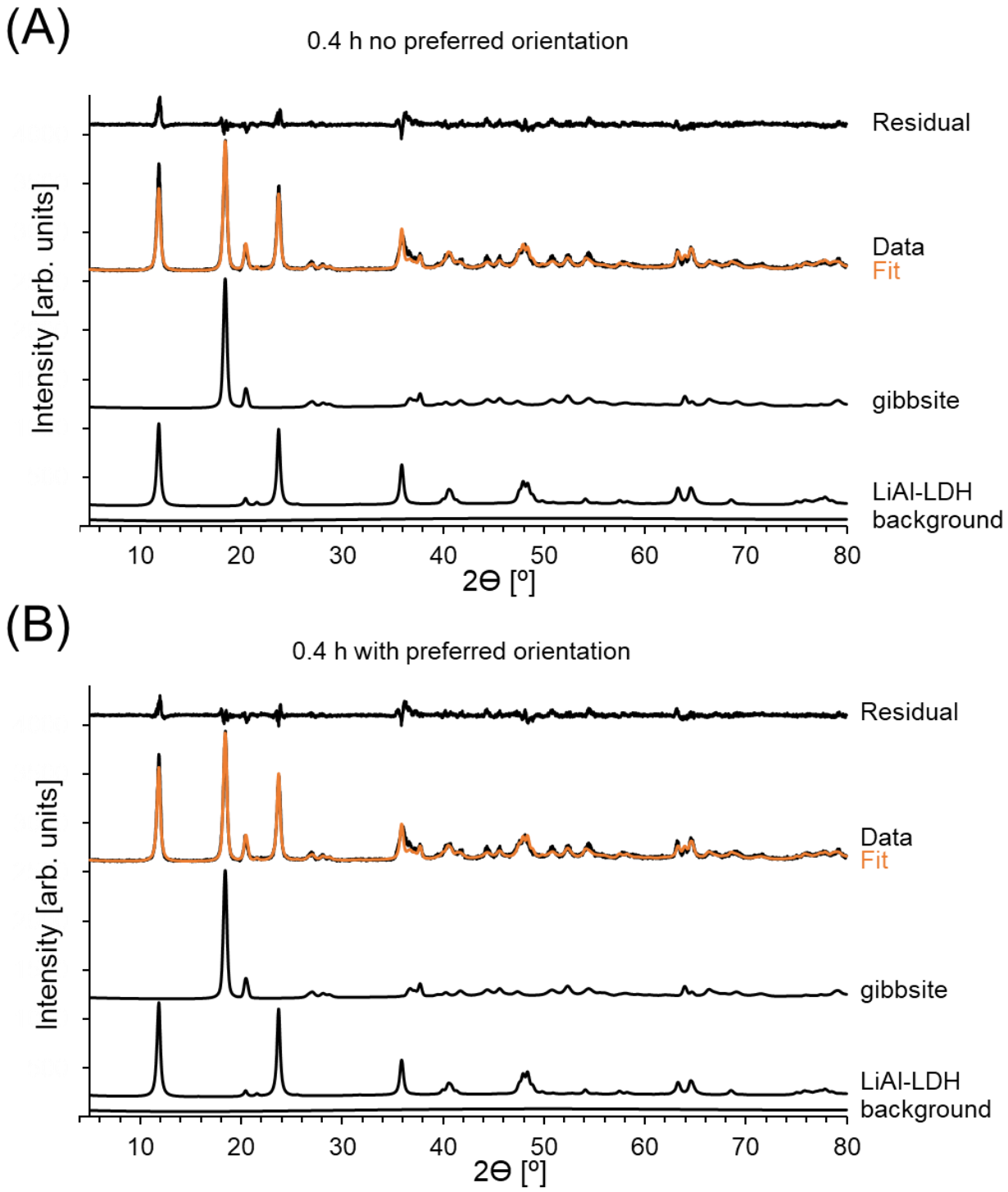

Figure S8. A typical fit of XRD patterns during the formation of LiAl-LDH [$Li(Al(OH)_3)_2OH{\cdot}2H_2O$] from gibbsite ($\alpha$-$Al(OH)_3$) in 3 M LiOH in D_2O. (A) The fit obtained with no preferential orientation. (B) The fits obtained with preferential orientation included. Fits were produced in TOPAS (v5).

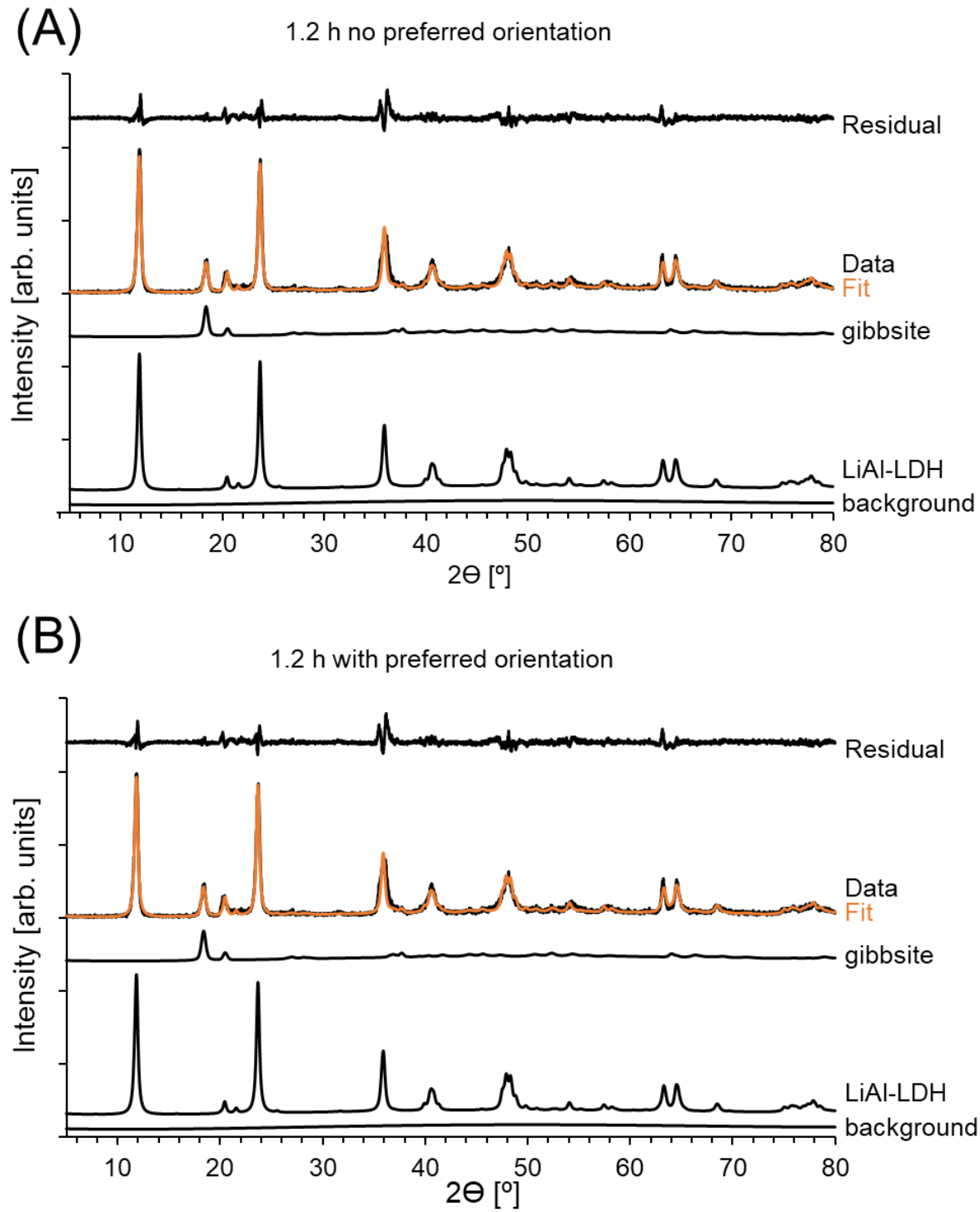

Figure S9. A typical fit of XRD patterns during the formation of LiAL-LDH [$Li(Al(OH)_3)_2OH{\cdot}2H_2O$] from gibbsite ($\alpha$-$Al(OH)_3$) in 3 M LiOH in D_2O. (A) The fit obtained with no preferential orientation. (B) The fits obtained with preferential orientation. Fits were produced in TOPAS (v5).

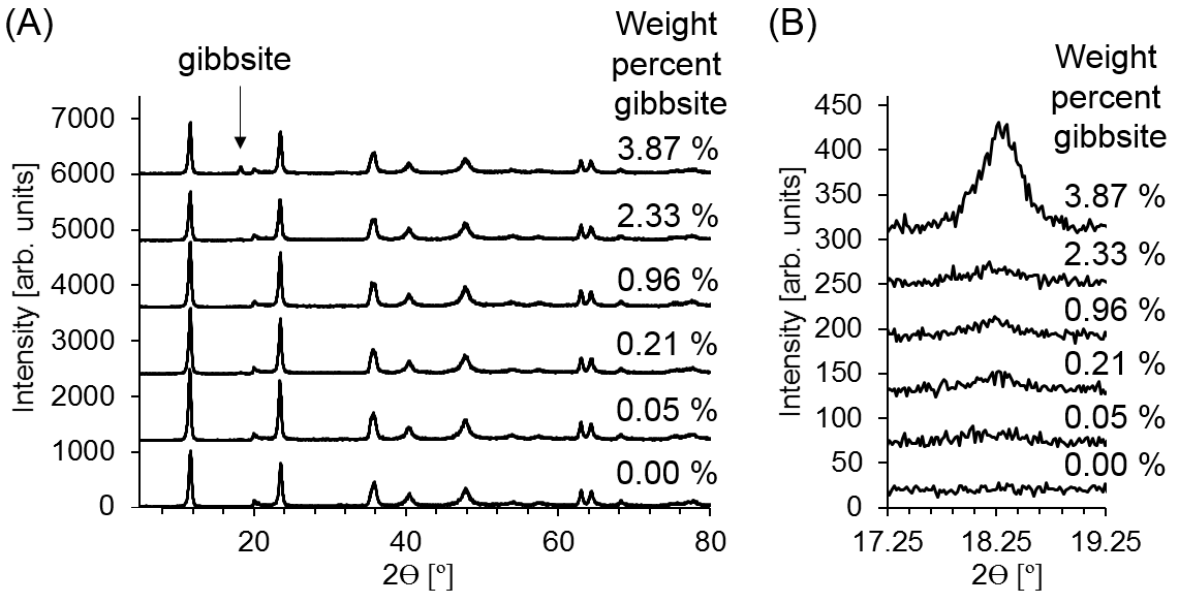

Figure S10. (A) XRD patterns of a series of mixtures of gibbsite and LiAl-LDH prepared to determine the limit of detection on the Philips X'pert Multi-Purpose diffractometer (MPD) (PANAlytical Almelo, The Netherlands), equipped with a fixed Cu anode operating at 40 mA and 50 kV. The limit of detection is ca. 3 wt%. Only the (002) peak of gibbsite is detected (marked with an arrow). (B) Magnification of the (002) peak of gibbsite in the 2Θ region between 17.25 and 19.25º.

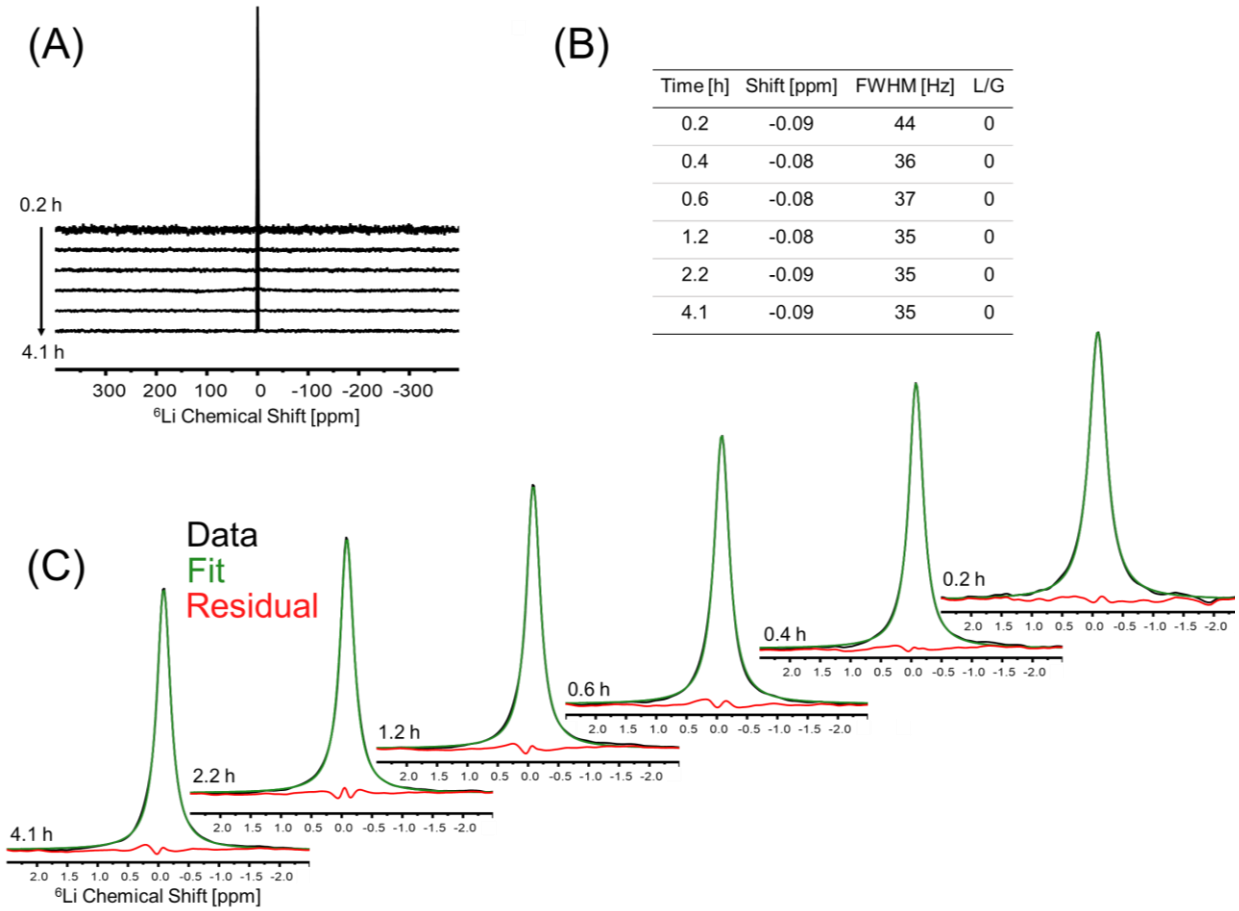

Time [h]	Shift [ppm]	FWHM [Hz]	L/G
0.2	-0.09	44	0
0.4	-0.08	36	0
0.6	-0.08	37	0
1.2	-0.08	35	0
2.2	-0.09	35	0
4.1	-0.09	35	0

Figure S11. (A) ^{6}Li MAS NMR collected at 20.0 T of the harvested solid samples showing the full spectral width. (B) Gaussian line shape parameters for the ^{6}Li spectra. (C) The corresponding fit and residual are shown for each of the ^{6}Li spectra.

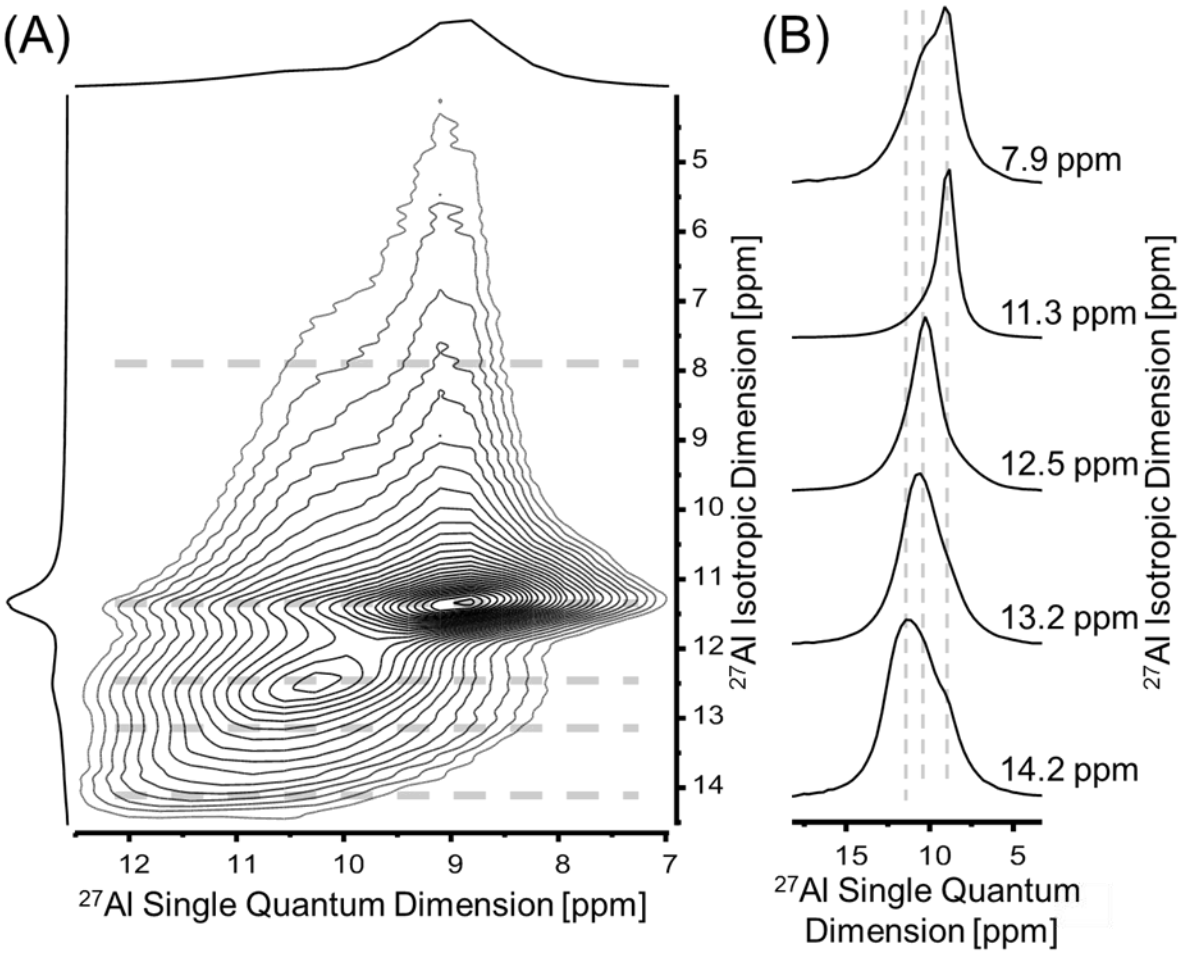

Figure S12. (A) ^{27}Al 3QMAS NMR at 20.0 T acquired using a 3.2 mm magic angle spinning MAS probe operating at a spin rate of 13.2 kHz. The spectra were acquired using the z-filter, ^{27}Al 3QMAS pulse sequence. The pulse widths, P_1, P_2, and P_3 were 6, 2, and 30 µs, respectively and 1104 transients were acquired. The recycle delay (d1) was 0.2 s, and spectra were acquired with 80 evolution increments and a 10.2 ms acquisition time. The spectral width for the F_2 (acquisition) and F_1 (evolution) dimension were 429 and 66 kHz, respectively. (B) Representative slices parallel to the single quantum dimension (F_2). The sample was prepared by vortex mixing 0.5 M gibbsite ($Al(OH)_3$) in 3 M LiOH in D_2O for 1 h in an N_2-filled glove box. The product was washed with D_2O three times using a centrifuge also located within the glovebox. The washed product was then dried for 3 days at room temperature and briefly homogenized with a mortar and pestle in the glovebox prior NMR analysis. For this sample, no signal intensity in the T_d region (80 - 70 ppm) nor the penta coordinated Al region was detected. The spectra reveal a well resolved peak at F_1 = 11.3 ppm corresponding to the emerging LiAl-LDH phase. Despite the occurrence of two Al sites in gibbsite, peaks corresponding to gibbsite site 1 and site 2 are not resolved. We suggest that the presence of resonances of Al^{3+} O_h sites proximal to Al^{3+} and/or Li^+ defects and vacancies overlap with those of the original gibbsite. We hypothesize that magnetic field strengths greater than 20.0 T are needed to spectroscopically distinguish the residual gibbsite sites from the Al^{3+} sites proximal to defects.

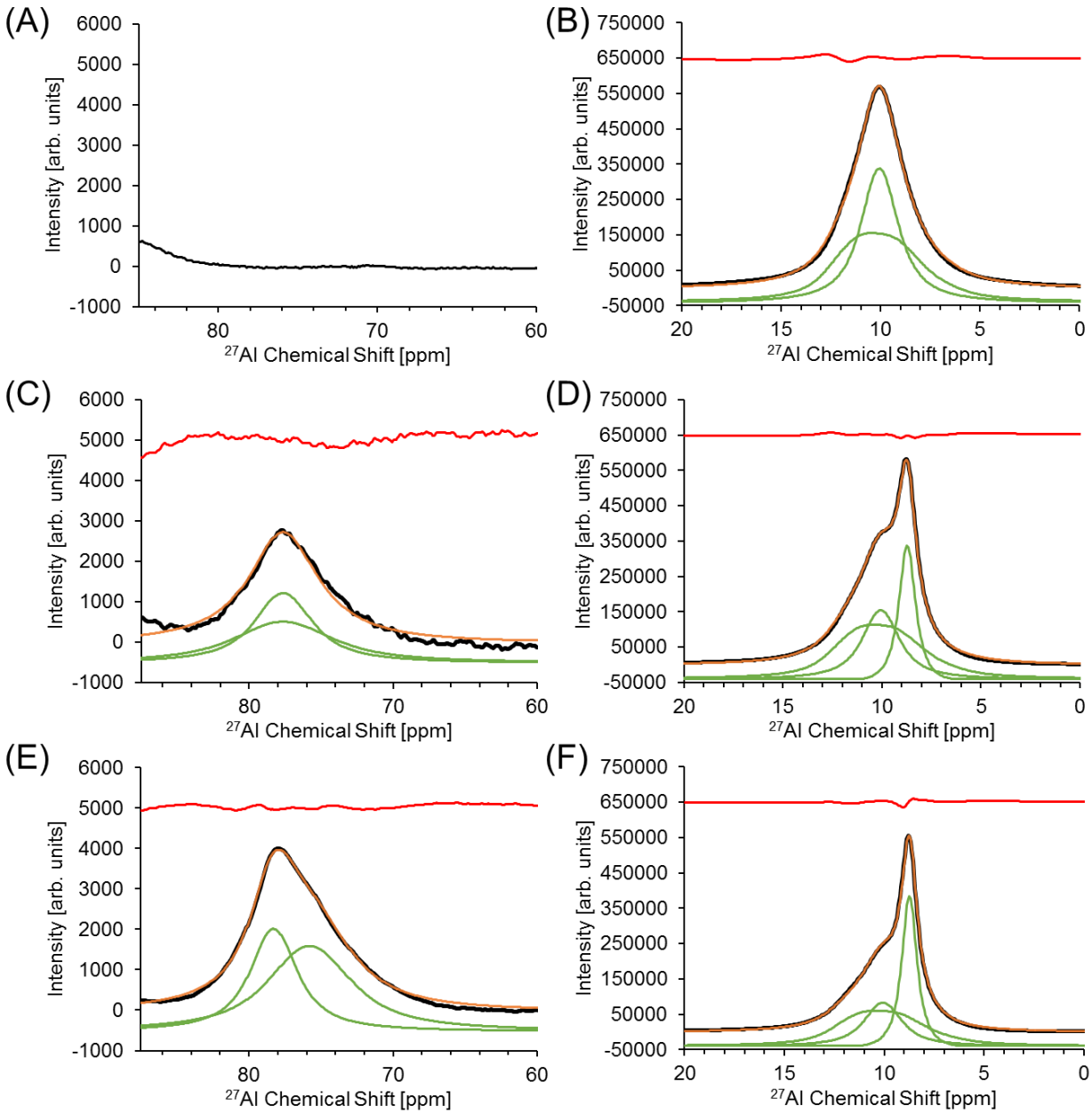

Figure S13. ^{27}Al MAS NMR spectra at 20.0 T where the data is denoted in black, the sum of the line shapes is denoted in orange, the residual is offset in red, and the individual line shapes are offset in green. Line shapes were generated with DMFIT (release #20180327). (A) Tetrahedral region of starting gibbsite (B) Octahedral Al region of starting gibbsite (C) Tetrahedral region after 0.2 h reaction (D) Octahedral Al region after 0.2 h reaction (E) Tetrahedral region after 0.4 h reaction (F) Octahedral Al region after 0.4 h reaction. For a summary of the quadrupolar coupling parameters, see Table S1.

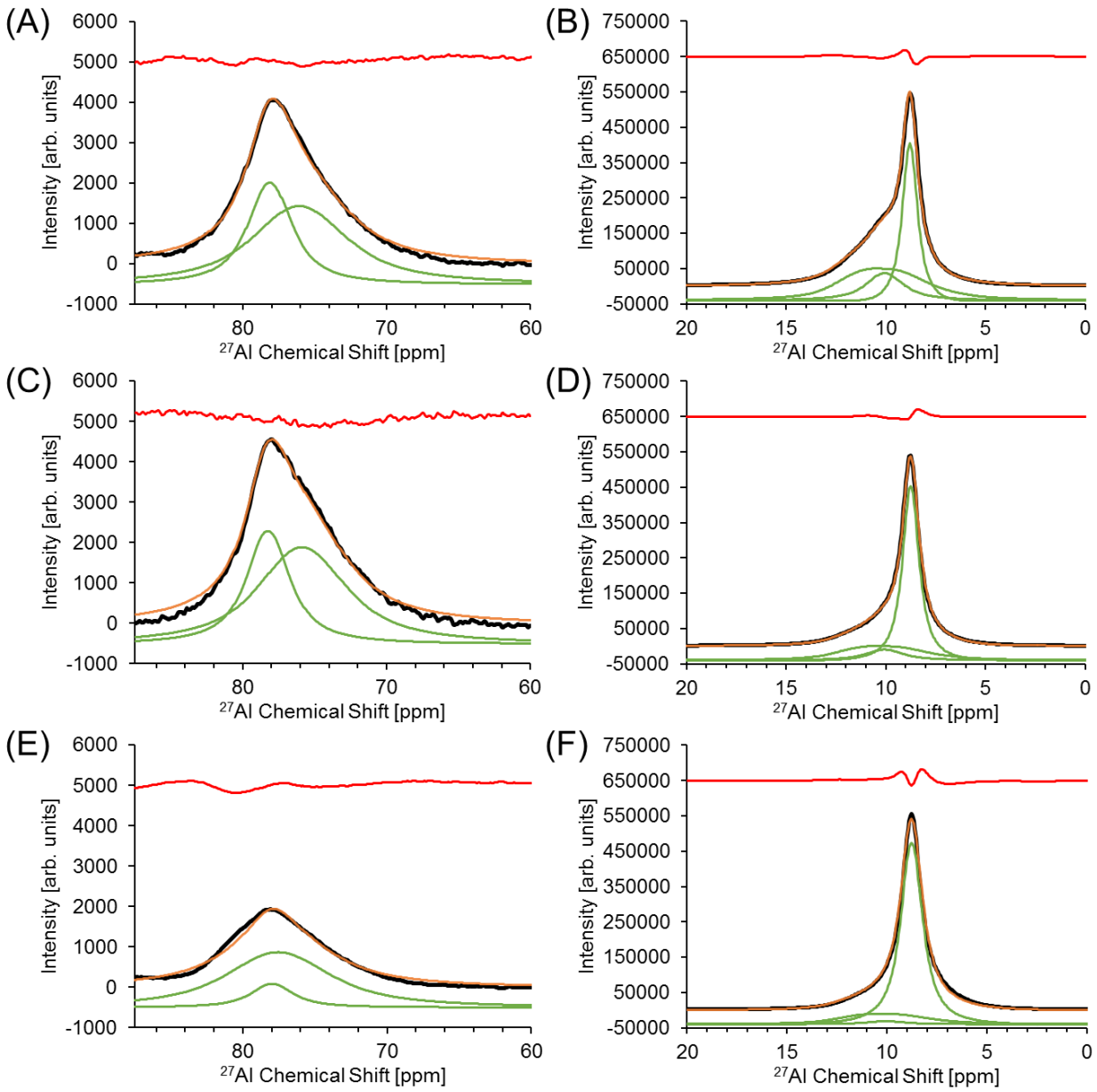

Figure S14. ^{27}Al MAS NMR spectra at 20.0 T where the data is denoted in black, the sum of the line shapes is denoted in orange, the residual is offset in red, and the individual line shapes are offset in green. Line shapes were generated with DMFIT (release #20180327). (A) Tetrahedral region after 0.6 h reaction (B) Octahedral Al region after 0.6 h reaction (C) Tetrahedral region after 1.2 h reaction (D) Octahedral Al region after 1.2 h reaction (E) Tetrahedral region after 2.2 h reaction (F) Octahedral Al region after 2.2 h reaction. For a summary of the quadrupolar coupling parameters, see Table S1.

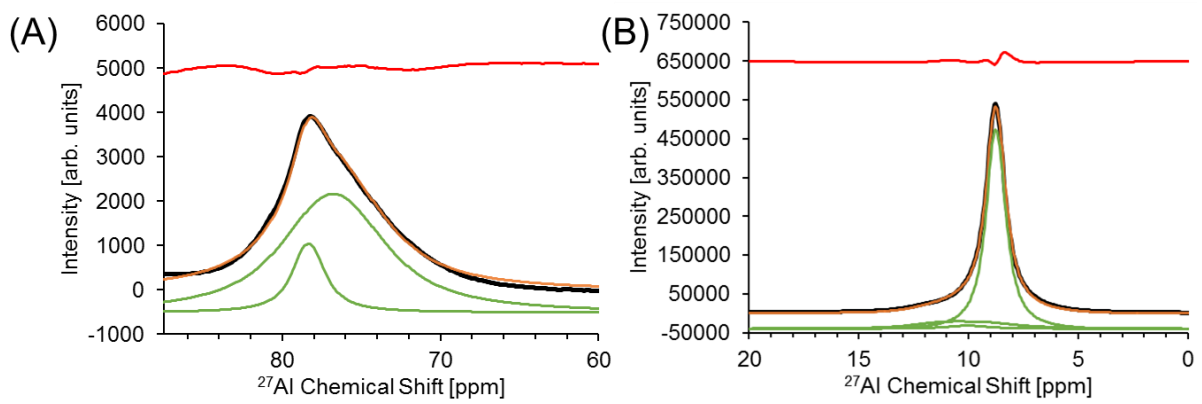

Figure S15. ^{27}Al MAS NMR spectra at 20.0 T where the data is denoted in black, the sum of the line shapes is denoted in orange, the residual is offset in red, and the individual line shapes are offset in green. Line shapes were generated with DMFIT (release #20180327). (A) Tetrahedral region after 4.1 h reaction (B) Octahedral Al region after 4.1 h reaction. For a summary of the quadrupolar coupling parameters, see Table S1.

Table S1. Tabulated ^{27}Al MAS NMR (20.0 T) Quadrupolar Coupling Parameters

	Peak	Integral [%]	Shift [ppm]	Cq [MHz]	etaQ	Lb [ppm]	Species
0 h	Octa Al 1	48.3	10.75	2.2	0.70	1.92	Gibbsite
	Octa Al 2	51.7	12.97	4.7	0.40	2.16	Gibbsite
	Peak	Integral [%]	Shift [ppm]	Cq [MHz]	etaQ	Lb [ppm]	Species
0.2 h	Octa Al 1	22.7	8.89	1.0	0.98	1.00	LiAl-LDH
	Octa Al 2	28.86	10.75	2.2	0.70	1.92	Gibbsite
	Octa Al 3	47.34	12.97	4.7	0.40	2.16	Gibbsite
	Tetra Al 1	0.55	79.02	3.3	0.46	4.22	--
	Tetra Al 2	0.54	80.39	4.1	1.00	6.76	--
	Peak	Integral [%]	Shift [ppm]	Cq [MHz]	etaQ	Lb [ppm]	Species
0.4 h	Octa Al 1	32.93	8.93	1.1	0.99	0.86	LiAl-LDH
	Octa Al 2	24.23	10.75	2.2	0.70	1.92	Gibbsite
	Octa Al 3	40.72	12.97	4.7	0.40	2.16	Gibbsite
	Tetra Al 1	1.25	78.03	3.8	0.92	5.84	--
	Tetra Al 2	0.86	79.32	2.8	0.41	3.51	--
	Peak	Integral [%]	Shift [ppm]	Cq [MHz]	etaQ	Lb [ppm]	Species
0.6 h	Octa Al 1	38.89	8.97	1.1	0.92	0.88	LiAl-LDH
	Octa Al 2	17.19	10.75	2.2	0.70	1.92	Gibbsite
	Octa Al 3	41.51	12.97	4.7	0.40	2.16	Gibbsite
	Tetra Al 1	1.5	78.84	4.1	0.99	6.44	--
	Tetra Al 2	0.91	79.38	2.8	0.91	3.04	--
	Peak	Integral [%]	Shift [ppm]	Cq [MHz]	etaQ	Lb [ppm]	Species
1.2 h	Octa Al 1	64.12	9.00	1.4	0.00	0.89	LiAl-LDH
	Octa Al 2	8.63	10.75	2.2	0.70	1.92	Gibbsite
	Octa Al 3	23.75	12.97	4.7	0.40	2.16	Gibbsite
	Tetra Al 1	2.21	78.4	4.0	0.98	6.06	--
	Tetra Al 2	1.29	79.3	2.9	0.36	3.12	--
	Peak	Integral [%]	Shift [ppm]	Cq [MHz]	etaQ	Lb [ppm]	Species
2.2 h	Octa Al 1	80.06	9.13	1.7	0.00	1.14	LiAl-LDH
	Octa Al 2	2.23	10.75	2.2	0.70	1.92	Gibbsite
	Octa Al 3	16.09	12.97	4.7	0.40	2.16	Gibbsite
	Tetra Al 1	0.24	79.08	2.8	0.69	2.99	--
	Tetra Al 2	1.38	80.49	4.3	0.96	7.14	--

	Peak	Integral [%]	Shift [ppm]	Cq [MHz]	etaQ	Lb [ppm]	Species
4.1 h	Octa Al 1	81.4	9.07	1.6	0.00	0.93	LiAl-LDH
	Octa Al 2	2.56	10.75	2.2	0.70	1.92	Gibbsite
	Octa Al 3	12.56	12.97	4.7	0.40	2.16	Gibbsite
	Tetra Al 1	0.55	79.04	2.4	0.11	2.16	--
	Tetra Al 2	2.92	79.41	4.0	0.99	6.36	--

Note: Resonances of Al^{3+} O_h sites proximal to defects and vacancies may overlap with those of the original gibbsite (Octa Al 2 and Octa Al 3). Quadrupolar line shape parameters in the ^{27}Al MAS NMR spectra collected at 20.0 T were evaluated with DMFIT (release #20180327), in which line shapes were estimated with the Qmas 1/2 model, which assumes an infinite spinning rate.

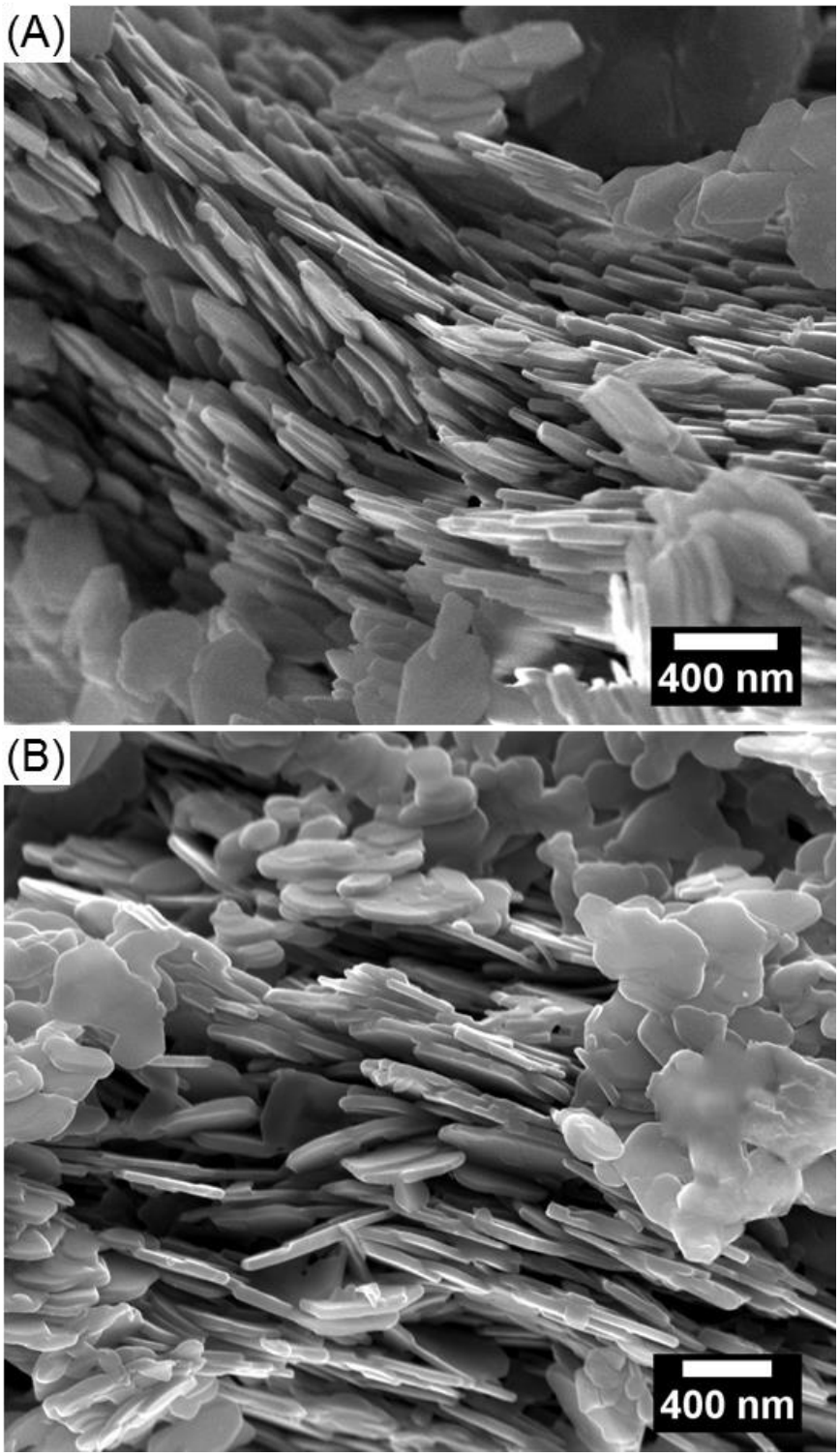

Figure S16. SEM images of the initial gibbsite and the solids harvested from dispersing 0.5 M gibbsite in 3 M LiOH in D_2O. (A) The unreacted gibbsite nanoplates and (B) the product after 4.1 h reaction, $Li[Al(OH)_3)]_2OH{\cdot}2H_2O$. The micrograph shown in (B) is reproduced from the main text.